

## THE INTERSTELLAR C-H STRETCHING BAND NEAR 3.4 MICRONS: CONSTRAINTS ON THE COMPOSITION OF ORGANIC MATERIAL IN THE DIFFUSE INTERSTELLAR MEDIUM

S. A. SANDFORD,<sup>1,2</sup> L. J. ALLAMANDOLA,<sup>1,2</sup> A. G. G. M. TIELENS,<sup>2</sup> K. SELLGREN,<sup>1,3</sup> M. TAPIA,<sup>1,4</sup>  
 & Y. PENDLETON<sup>2</sup>

Received 1990 August 16; accepted 1990 October 3

### ABSTRACT

To better constrain and quantify the composition of material in the diffuse interstellar medium (ISM), absorption spectra between 3600 and 2700  $\text{cm}^{-1}$  (2.8 and 3.7  $\mu\text{m}$ ) have been taken of objects which have widely varying amounts of visual extinction along different lines of sight. The spectra of these objects contain a broad feature centered at  $\sim 3300 \text{ cm}^{-1}$  ( $\sim 3.0 \mu\text{m}$ ), attributed to O-H stretching vibrations, and/or a feature near 2950  $\text{cm}^{-1}$  (3.4  $\mu\text{m}$ ) attributed to C-H stretching vibrations. The lack of correlation between the strengths of these two bands indicates that they do not arise from the same molecular carrier.

The features in the 3100–2700  $\text{cm}^{-1}$  (3.2–3.7  $\mu\text{m}$ ) region fall into one of two classes. We attribute the first class of features to material in the diffuse ISM on the basis of the similarity between the band profiles along the very different lines of sight to Galactic center source IRS 7 and VI Cygni #12. Similar features are also reported for Galactic center source IRS 3, Ve 2–45, and AFGL 2179. Higher resolution spectra of the objects OH 01–477 and T629–5, which are known to be M stars, are dominated by a series of narrow bands in this region. These bands are largely due to OH in the stars' photospheres. While the spectra of OH 01–477 and T629–5 are likely to contain C-H absorption from diffuse ISM dust, the strength of the overlapping photospheric OH features presently prevents us from quantifying the depths of the interstellar C-H feature towards these objects.

The interstellar feature for Galactic center source IRS 7 has subpeaks near 2955, 2925, and 2870  $\text{cm}^{-1}$  ( $\pm 5 \text{ cm}^{-1}$ ), which we attribute to C-H stretching vibrations in the  $-\text{CH}_2-$  and  $-\text{CH}_3$  groups of aliphatic hydrocarbons. These band positions fall within 5  $\text{cm}^{-1}$  of the values normal for saturated aliphatics. The absence of a distinct band near 2855  $\text{cm}^{-1}$  suggests that the material contains small amounts of electronegative groups like  $-\text{O}-\text{H}$  or  $-\text{C}\equiv\text{N}$ . The relative strengths and profiles of the 2955 and 2925  $\text{cm}^{-1}$  features towards five objects suggests an average diffuse ISM line-of-sight  $-\text{CH}_2-/-\text{CH}_3$  ratio of about 2.5, indicating the presence of relatively complex organic materials. The strengths of the subpeaks at 2925 and 2955  $\text{cm}^{-1}$ , due to  $-\text{CH}_2-$  and  $-\text{CH}_3$  groups, respectively, correlate with visual extinction, strongly suggesting that the C-H stretching band is a general feature of the material along different lines of sight in the diffuse ISM. We find average ratios of  $A_{\nu}/\tau_{(2925 \text{ cm}^{-1})} = 240 \pm 40$  and  $A_{\nu}/\tau_{(2955 \text{ cm}^{-1})} = 310 \pm 90$  for the objects we have observed. We deduce that 2.6%–35% of the cosmic carbon in the ISM is tied up in the carrier of this band with the most likely value falling near 10%.

The interstellar C-H band is remarkably similar to the feature in lab residues produced by irradiating analogs of dense molecular cloud ices. This is consistent with a model in which the hydrocarbon component in the diffuse interstellar medium consists of complex hydrocarbons containing aliphatic side chains and bridges which are produced in dense molecular clouds and subsequently modified in the diffuse medium.

*Subject headings:* infrared: spectra — interstellar: grains — interstellar: molecules

### 1. INTRODUCTION

The nature of dust in the diffuse interstellar medium (ISM) has been the subject of much controversy and speculation. General parameters such as size and shape have been constrained using the UV-visual portion of the extinction curve and polarization measurements. These, in conjunction with cosmic abundance constraints and the optical properties of several materials, have been used to place some constraints on dust composition (see e.g., Greenberg 1989; Mathis 1989; Williams 1989, and references therein). Mathis and coworkers

have proposed several models in which the dust population is assumed to consist of mixtures of silicate and graphite materials (Mathis, Rumpl, & Nordsieck 1977; Mathis & Whiffen 1989). These particles are thought to be produced in outflows from late-type giants and modified in the interstellar medium. Greenberg and coworkers (see Greenberg 1978; Greenberg & Hong 1974; Greenberg & Chlewicki 1983) have suggested that the visual extinction is dominated by core-mantle grains in which the cores are thought to consist of silicate materials ejected by late-type stars and the mantles consist of a complex molecular mixture formed by UV photolysis of simple ices accreted in dense clouds. Jones, Duley, & Williams (1987, and references therein) have proposed a mixture of silicate grains and hydrogenated amorphous carbons (HACs) having various amounts of hydrogenation. Recent reviews of these models, and pertinent references can be found in Greenberg (1989), Mathis (1989), and Williams (1989).

<sup>1</sup> Visiting Astronomer, Infrared Telescope Facility, which is operated by the Univ. of Hawaii under contract with the National Aeronautics and Space Administration.

<sup>2</sup> NASA-Ames Research Center, Mail Stop 245-6, Moffett Field, CA 94035.

<sup>3</sup> Institute for Astronomy, University of Hawaii, Honolulu, HI 96822, and Department of Astronomy, Ohio State University, 174 West 18th Avenue, Columbus, OH 43210.

<sup>4</sup> Instituto de Astronomia, UNAM, P.O. Box 73027, San Ysidro, CA 97073.

The detection of absorption bands near  $3300$  and  $2950\text{ cm}^{-1}$  ( $3.0$  and  $3.4\text{ }\mu\text{m}$ ) by Soifer, Russell, & Merrill (1976), Willner et al. (1979), and Wickramasinghe & Allen (1980) in the spectrum of Galactic center source IRS 7 (hereafter called GC IRS 7) has led to many follow-up observations and analyses because the features along this line of sight have been thought to be dominated by dust in the diffuse interstellar medium (Allen & Wickramasinghe 1981; Willner & Pipher 1982; Jones, Hyland, & Allen 1983; Wickramasinghe & Allen 1983; Allamandola 1984; Butchart et al. 1986; Tielens & Allamandola 1987; McFadzean et al. 1989). These features are generally interpreted as being due to O-H and C-H stretching vibrations, respectively. Unfortunately, until very recently no other lines of sight through the diffuse medium showed clear-cut evidence for these features, and no firm conclusions regarding the compositions of diffuse cloud dust could be drawn. Quite recently McFadzean et al. (1989) have reported  $3450\text{--}2630\text{ cm}^{-1}$  ( $2.90\text{--}3.80\text{ }\mu\text{m}$ ) spectra of several Galactic center sources and note that the broad O-H feature near  $3300\text{ cm}^{-1}$  ( $3.0\text{ }\mu\text{m}$ ) varies in strength from source to source. It is difficult to ascertain how much of this absorption arises from material local to the Galactic center and how much (if any) arises from the intervening ISM. This uncertainty, first discussed by Soifer, Russell, & Merrill in 1976, underscores the need for probes of the diffuse medium along other lines of sight.

Another object for which the C-H stretch region near  $2950\text{ cm}^{-1}$  ( $3.4\text{ }\mu\text{m}$ ) has been the focus of attention is VI Cygni # 12. This object is known to be obscured by approximately 10 magnitudes of interstellar extinction. If the same ratio for  $A_v/\tau_{\text{(CH)}}$  holds as for the Galactic center sources, a band should be detectable near  $2950\text{ cm}^{-1}$  ( $3.4\text{ }\mu\text{m}$ ; Tielens & Allamandola 1987). Although the infrared spectrum of this object has been known for some time (Gillett et al. 1975), the signal-to-noise ratio required for the confident detection of the weak absorption feature was not achieved until the recent work of Adamson, Whittet, & Duley (1990). In this work a broad feature attributable to C-H was definitely detected and a discussion of the ramifications if HAC is responsible is given.

In order to further our understanding of the composition and history of dust in the diffuse interstellar medium, we have undertaken an observing and analysis program which covers the  $3450\text{--}2700\text{ cm}^{-1}$  ( $2.89\text{--}3.70\text{ }\mu\text{m}$ ) region of various objects

thought to be probes of diffuse medium dust. The observational aspect of this program emphasizes high quality, good signal-to-noise spectra in order to determine the origin of the O-H and C-H features (i.e., whether they are interstellar or not), the quantities and compositions of the carrier materials, and the relationship of these spectral features to other observable quantities such as extinction and optical depth of the silicates.

## 2. OBSERVATIONS AND DATA REDUCTION

The observations were made using the 3 m NASA Infrared Telescope Facility (IRTF) on Mauna Kea during 1989 August 6–8. Spectra were obtained using the LN<sub>2</sub>-cooled, 32 InSb detector cooled-grating array spectrometer (CGAS). The performance and configuration of this instrument is described in more detail in Tokunaga, Smith, & Irwin (1987). At the time of operation, detectors 1, 2, 13, and 32 were not working reliably on the CGAS and the output from these detectors was not used. We used grating A, which has 75 grooves  $\text{mm}^{-1}$  and provides a resolution of  $0.018\text{ }\mu\text{m}$  per detector [ $\lambda/\Delta\lambda = 160\text{--}210$  over the  $3570\text{--}2770\text{ cm}^{-1}$  ( $2.80\text{--}3.61\text{ }\mu\text{m}$ ) range], and grating B, which has 300 grooves  $\text{mm}^{-1}$  and a resolution of  $0.004\text{ }\mu\text{m}$  per detector [ $\lambda/\Delta\lambda = 790\text{--}880$  over the  $3100\text{--}2800\text{ cm}^{-1}$  ( $3.25\text{--}3.55\text{ }\mu\text{m}$ ) range]. Both gratings were used in first order. Wavelength calibration was achieved in second order by comparison with the  $5901\text{ cm}^{-1}$  ( $1.65\text{ }\mu\text{m}$ ) line of an Argon lamp. The detector spacing on the CGAS provides one detector per resolution element. In several cases, additional spectra were taken at half-channel shifts to provide full Nyquist sampling. The CGAS has a fixed aperture of  $2.7$  diameter.

Sky subtraction was accomplished through alternately measuring the object and nearby sky by nodding the telescope. Correction for atmospheric absorption and flux calibration was accomplished by comparison with nearby bright stars whose spectra were measured through similar air masses on the same night that the object was observed (usually within an hour). No further telluric extinction corrections were made to the data since the average air masses of our objects and their comparison bright stars nowhere differed by more than 0.03 air masses.

Details of the objects and their comparison stars are summarized in Table 1. Included are the color temperatures and  $L$

TABLE 1  
SUMMARY OF OBSERVATIONS

Object	Object R.A. (1950)	Object Decl. (1950)	Comparison Star and Spectral Type	Comparison Star Color Temp (K)	Comparison Star $L$ -Magnitude	Throw
Galactic center IRS 3	17 <sup>h</sup> 42 <sup>m</sup> 29 <sup>s</sup> .1	−28°59′14″.9	BS 6692 (B3IV)	15500	6.3	225" EW
Galactic center IRS 7						
Grating A	17 42 29.3	−28 59 13.1	BS 6692 (B3IV)	15500	6.3	225 EW
Grating B			BS 6616 (F7II)	6000	2.6	225 EW
OH 01−477						
Grating A	17 46 12.5	−27 40 49.6	BS 6692 (B3IV)	15500	6.3	225 EW
Grating B			BS 6616 (F7II)	6000	2.6	225 EW
Ve 2−45	17 59 00.9	−23 37 35.2	BS 6700 (B9V)	10600	4.9	30 EW
AFGL 2179	18 28 56.8	−10 01 23.3	BS 7094 (F2Ib)	7200	4.4	30 EW
T629−5						
Grating A	18 30 23.0	−08 44 16.6	BS 7094 (F2Ib)	7200	4.4	30 EW
Grating B			BS 7236 (B9Vn)	10600	3.6	30 EW
VI Cygni #12	20 30 53.4	+41 03 51.6	BS 8028 (A1Vn)	9120	3.86	30 EW
VI Cygni IRS 7	20 33 39.6	+41 22 15.8	BS 8028 (A1Vn)	9120	3.86	30 EW
OH 32.8−0.3	18 49 48.1	−00 17 53.7	BS 7269 (B5Vn)	13800	7.2	30 EW

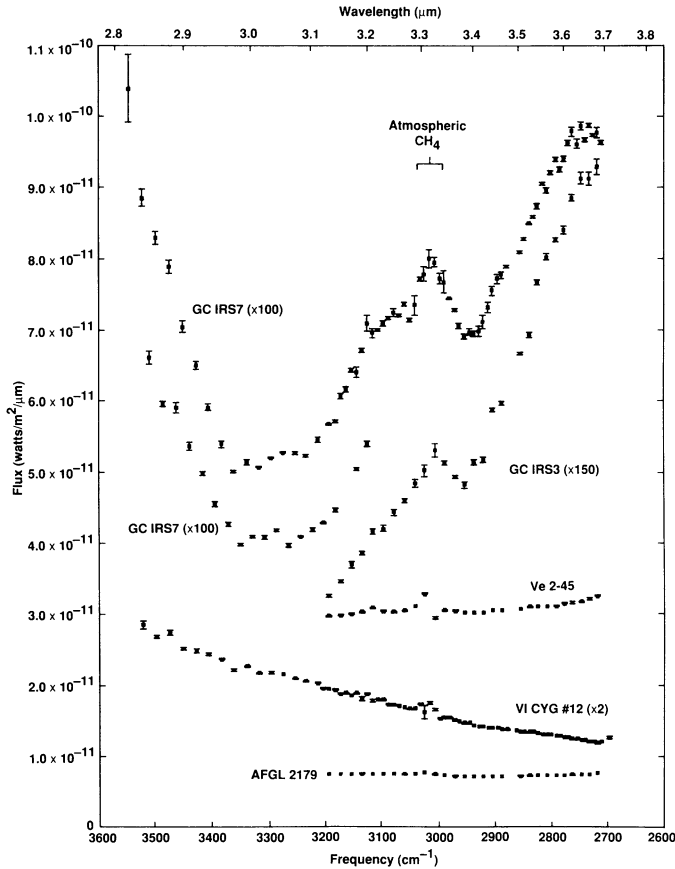


FIG. 1a

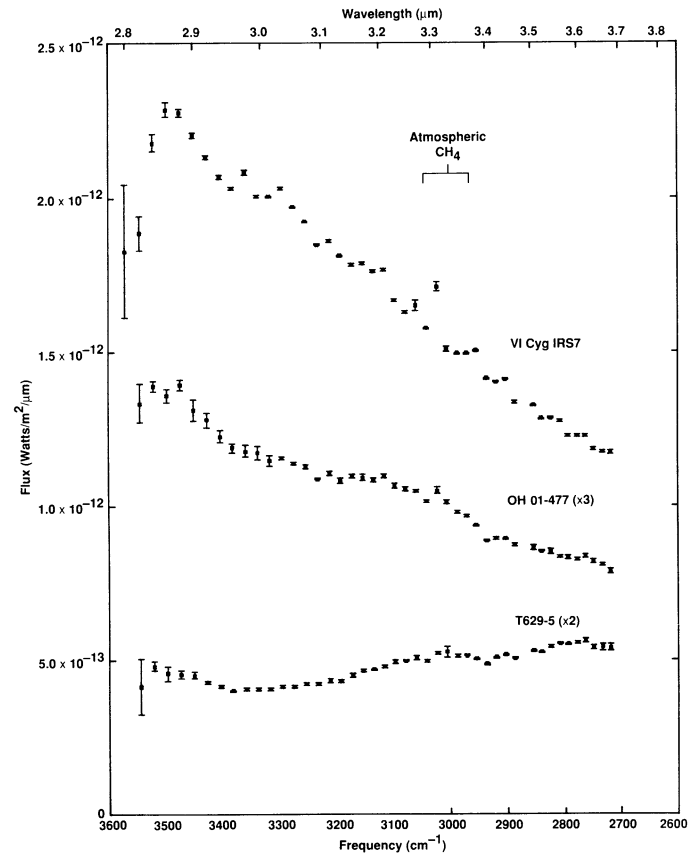


FIG. 1b

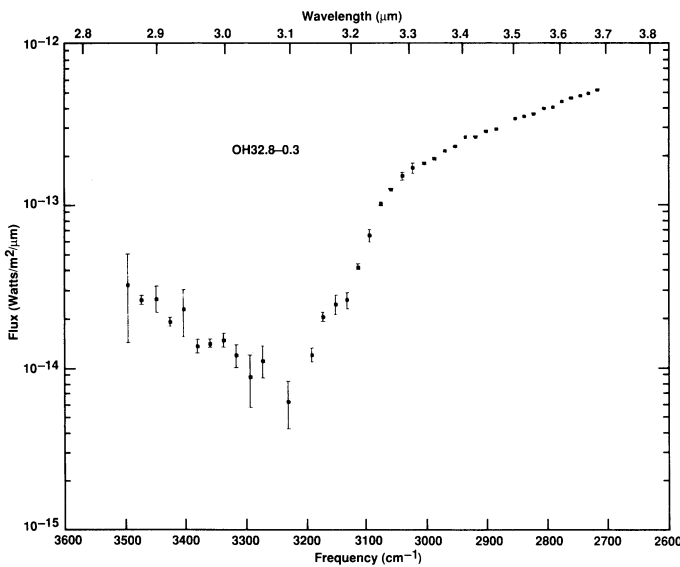


FIG. 1c

FIG. 1.—(a) Spectra of Galactic center sources IRS 7 and IRS 3, Ve 2–45, VI Cygni # 12, and AFGL 2179. These spectra have a resolution of  $0.018 \mu\text{m}$  per detector [ $\lambda/\Delta\lambda = 160\text{--}210$  over the  $3570\text{--}2770 \text{ cm}^{-1}$  ( $2.80\text{--}3.7 \mu\text{m}$ ) range]. In this and subsequent figures, points without error bars have errors smaller than the points themselves. The difference in flux levels of the two GC IRS 7 spectra reflect typical photometric uncertainties. For GC IRS 7 and VI Cygni # 12 spectra were double-sampled with a  $\frac{1}{2}$  channel shift from 3200 to 2700  $\text{cm}^{-1}$ . (b) Spectra of VI Cygni IRS 7, OH 01–477, and T629–5 at the same resolution as the spectra in Fig. 1a. (c) Spectrum of OH 32.8–0.3 at the same resolution as the spectra in Fig. 1a. Note that this spectrum has been plotted on a log scale.

magnitudes derived for the comparison stars used to reduce the data. Since  $L$  band photometry is not available for most of the comparison stars in this work, the  $L$  magnitudes used were determined by ratioing comparison star spectra to the spectrum of BS 8028 ( $v$  Cygni), which was assumed to have an  $L$  magnitude of 3.86 (IRTF Photometry Manual, 1986). The derived  $L$  magnitudes were then compared to those expected from known  $V$  magnitudes and spectral types to ensure the stars used were spectrally well-behaved. Fluxes are based on a 0.0 magnitude flux of  $7.3 \times 10^{-11} \text{ W m}^{-2} \mu\text{m}^{-1}$  at  $L$  ( $3.34 \mu\text{m}$ ; IRTF Photometry Manual, 1986). The resulting calculated fluxes were in reasonable agreement with published photometry values for all the objects except Ve 2–45 and AFGL 2179. The fluxes for our spectra of Ve 2–45 and AFGL 2179 shown in Figure 1a need to be multiplied by factors of 2.6 and 1.9, respectively, to be consistent with the broadband data (Pitault et al. 1983; Cohen & Vogel 1978).

As a final check, all the comparison star spectra taken at each grating setting were cross-compared to ensure that none of the spectral features reported here are due to features within the comparison star spectra themselves.

### 3. DATA AND RESULTS

#### 3.1. The Objects and Their Spectra

A summary of the objects we observed is presented below. Our spectra of these objects are shown in Figures 1a, 1b, 1c, 2, and 3. Since this work is concerned with weak spectral features due to diffuse interstellar material, the spectra were converted

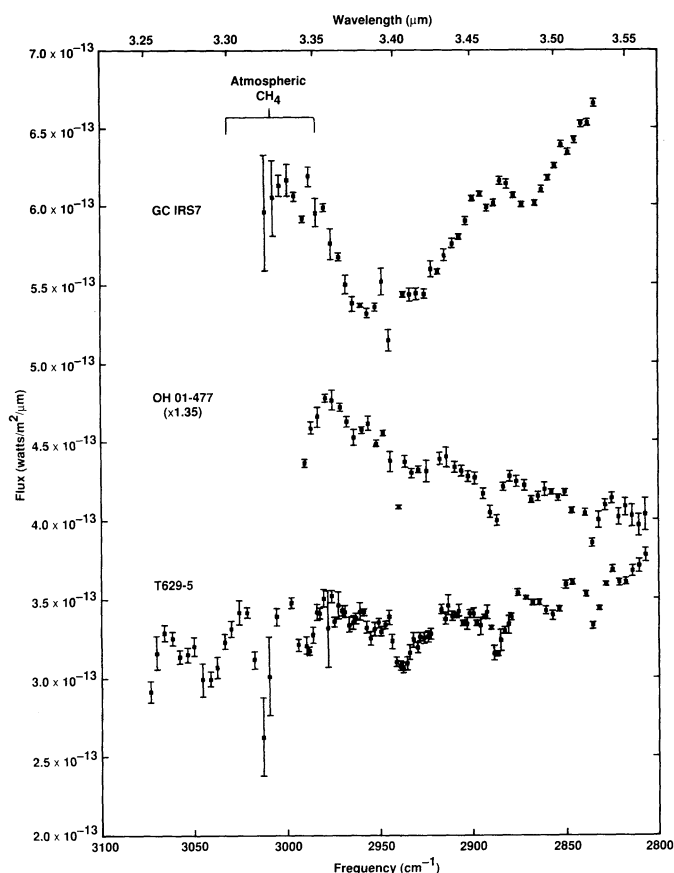


FIG. 2.—Spectra of Galactic center source GC IRS 7, OH 01-477, and T629-5. For GC IRS 7 and OH 01-477 the resolution is  $0.004 \mu\text{m}$  per detector [ $\lambda/\Delta\lambda = 790\text{--}880$  over the  $3100\text{--}2800 \text{ cm}^{-1}$  ( $3.25\text{--}3.55 \mu\text{m}$ ) range]. For T629-5 the spectrum was double-sampled with a  $\frac{1}{2}$  channel shift from  $2875$  to  $2975 \text{ cm}^{-1}$ .

into absorbance (optical depth) plots. This allows for straightforward intercomparison of the band profiles and strengths. Conversion of the spectra to absorbance requires that we define the “continuum” baselines under the features. In practice it is often difficult to uniquely define these baselines.

An example of this difficulty can be seen from the spectrum of the Galactic center source IRS 7 shown in Figure 3. For intercomparison of the O-H and C-H stretching features centered near  $3300 \text{ cm}^{-1}$  ( $3.0 \mu\text{m}$ ) and  $2950 \text{ cm}^{-1}$  ( $3.4 \mu\text{m}$ ), respectively, broad-band observations suggest that a linear continuum extending across both features is acceptable (Becklin et al. 1987b). For all but one of the low-resolution spectra which cover the  $3550\text{--}2700 \text{ cm}^{-1}$  ( $2.8\text{--}3.7 \mu\text{m}$ ) region containing both the O-H and C-H features, we have generated the absorbance plots assuming a linear baseline spanning both features. An example of the baseline used is given by the line of alternating dots and dashes in Figure 3. The baseline corrections for the one exception, VI Cygni #12, are discussed separately later in this section. The resulting absorbance plots can be found in Figure 4 and are useful for comparing the relative strength of the O-H and C-H features along the line of sight to these different objects.

Determination of the appropriate baseline under the C-H feature alone is more difficult since this feature often lies superposed on the long-wavelength side of the broad O-H

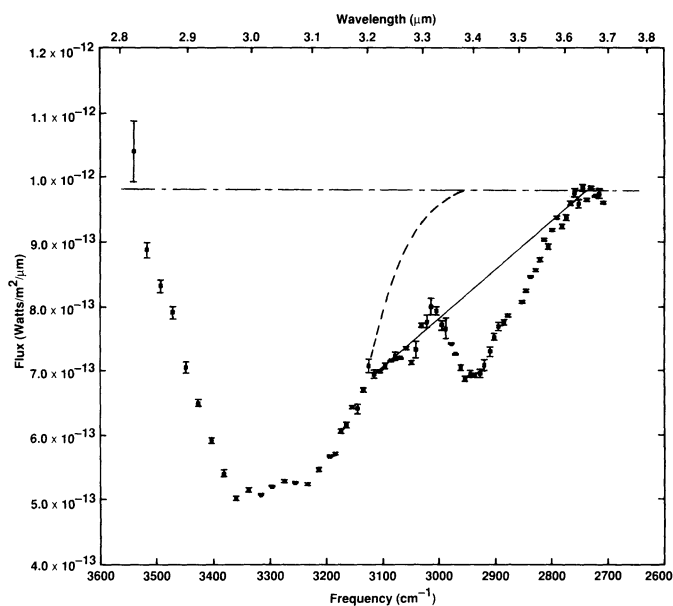


FIG. 3.—Spectrum of Galactic center source GC IRS 7. The various lines demonstrate possible baselines that can be used to generate absorbance (optical depth) plots. For the C-H feature near  $2950 \text{ cm}^{-1}$ , we have used the baseline given by the solid line to produce the absorbance spectra shown in Fig. 5a. It is clear that this baseline will yield conservative lower limits to the C-H absorption strength. The dot-dash line was used to produce the absorbance spectra in Fig. 4. The resolution is the same as that in Fig. 1a.

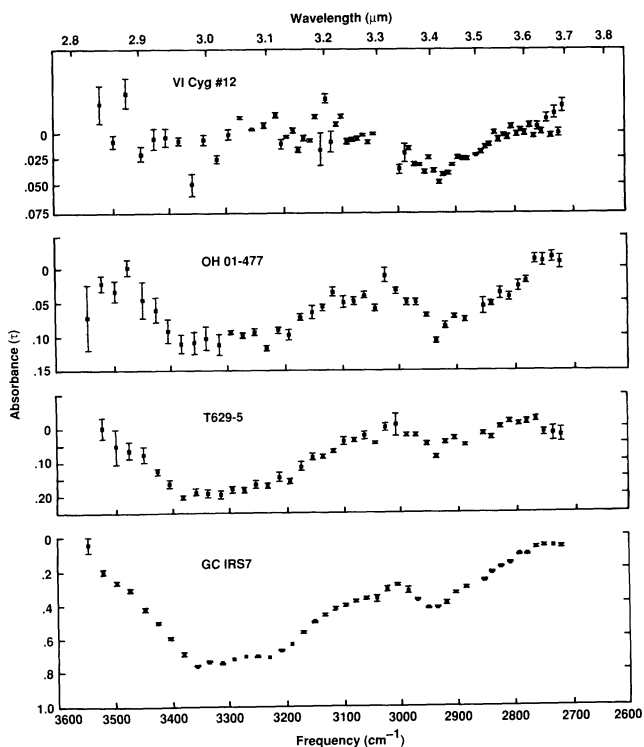


FIG. 4.—Absorbance (optical depth) plots for the  $3600\text{--}2600 \text{ cm}^{-1}$  ( $2.8\text{--}3.85 \mu\text{m}$ ) region of VI Cygni #12, OH 01-477, T629-5, and GC IRS 7. Except for VI Cygni #12, these plots were generated using a straight baseline like that given by the upper dot-dash line in Fig. 3. The baseline for VI Cygni #12 was generated numerically by fitting the entire data set to an exponential (see text). The resolution is the same as that in Fig. 1a.

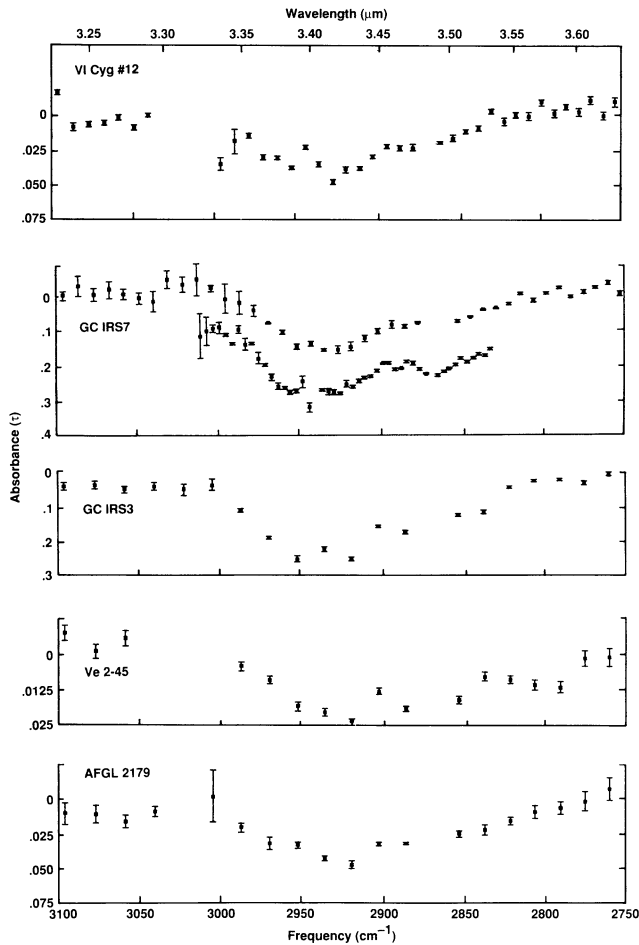


Fig. 5a

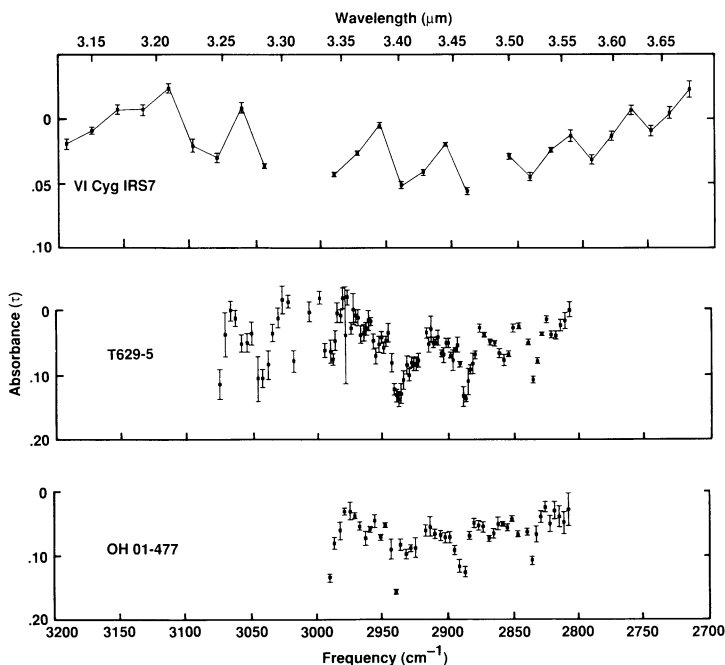


FIG. 5b

stretching feature centered near  $3300\text{ cm}^{-1}$  ( $3.0\text{ }\mu\text{m}$ ) (see Fig. 3). Possible extremes for the baseline under the C-H feature for the Galactic center source IRS 7 are represented by the dashed and solid lines in Figure 3. The dashed line was generated by simply assuming that the O-H feature is symmetric around  $3300\text{ cm}^{-1}$  ( $3.0\text{ }\mu\text{m}$ ) and that all the remaining absorption is due to the C-H feature, while the baseline represented by the solid line assumes a linear continuum between the data points near  $3100$  and  $2750\text{ cm}^{-1}$  ( $3.23$  and  $3.64\text{ }\mu\text{m}$ ). Since it is likely that the O-H stretching mode has a low-frequency wing (Hagen, Tielens, & Greenberg 1983), we have adopted the latter baseline for the production of the absorbance plots of the C-H feature (except for VI Cygni #12). It is clear from Figure 3 that the use of this baseline will result in an underestimate of the depth of the C-H feature for some objects. Thus, it should be kept in mind throughout this paper that *the strengths of the C-H features reported here represent conservative lower limits*. Comparison with the spectra of various O-H containing laboratory materials indicates that our conservative baselines may result in derived C-H feature strengths that are as much as 20%–30% low.

### 3.2. Galactic Center—GC IRS 7

Near-infrared spectra of GC IRS 7 reveal the presence of strong photospheric CO bands and this star has been classified as an M2I supergiant (Lebofsky, Rieke, & Tokunaga 1982; Sellgren et al. 1987). Various estimates of the interstellar visual extinction towards the inner 3 pc of the Galactic center generally agree on a value of about 31 mag (Becklin et al. 1978b; Rieke, Rieke, & Paul 1989; Henry, DePoy, & Becklin 1984; Sellgren et al. 1987; Wade et al. 1987). GC IRS 7 shows a total visual extinction of about 37 mag indicating an excess extinction of  $\sim 6$  mag compared to the other sources in the Galactic center, perhaps due to silicate dust grains in a circumstellar shell (Rieke, Rieke, & Paul 1989).

Our low- and high-resolution spectra of this source are shown in Figures 1a and 2, respectively. Comparison of the low- and high-resolution spectra shows good agreement in the spectral shape of the C-H feature in both spectra. The C-H stretch feature has been seen in the spectrum of GC IRS 7 before (see Jones, Hyland, & Allen 1983; Butchart et al. 1986) and is confirmed by our higher S/N and resolution data. We have converted our spectra of this object into baseline corrected absorbance (optical depth) plots which can be found in Figures 4 and 5a.

### 3.3. Galactic Center—IRS 3

The nature of Galactic center source IRS 3 is less clear. As suggested by Becklin et al. (1978a), it may be an OH/IR

FIG. 5.—(a) Absorbance (optical depth) plots for the  $3100\text{--}2750\text{ cm}^{-1}$  ( $3.23\text{--}3.64\text{ }\mu\text{m}$ ) region of VI Cygni #12, GC IRS 7, GC IRS 3, Ve 2–45, and AFGL 2179. Except for VI Cygni #12, these plots were generated using a straight baseline like that given by the solid line in Fig. 3 and thus represent lower limits to the optical depth of the C-H feature. The GC IRS 3, Ve 2–45, and AFGL 2179 spectra have resolutions of  $0.018\text{ }\mu\text{m}$  per detector. The spectrum of VI Cygni #12 and the top spectrum of GC IRS 7 were double-sampled with a  $\frac{1}{2}$  channel shift in this wavelength region. The lower spectrum of GC IRS 7 was taken at a resolution of  $0.004\text{ }\mu\text{m}$  per detector and has been displaced downward by 0.1 absorbance units for clearer display. (b) Absorbance (optical depth) plots for the  $3100\text{--}2750\text{ cm}^{-1}$  ( $3.23\text{--}3.64\text{ }\mu\text{m}$ ) region of VI Cygni IRS 7, T629–5, and OH 01–477. These plots were generated using a straight baseline like that given by the solid line in Fig. 3. The spectrum of VI Cygni IRS 7 has a resolution of  $0.018\text{ }\mu\text{m}$  per detector. The other two spectra have resolutions of  $0.004\text{ }\mu\text{m}$  per detector. The spectrum of T629–5 was double-sampled with a  $\frac{1}{2}$  channel shift from  $2875$  to  $2975\text{ cm}^{-1}$ .

star—an M giant embedded in a circumstellar shell. Because its nature and intrinsic colors are unknown, we have adopted a value of 31 mag, typical of the Galactic center region (Rieke, Rieke, & Paul 1989), for the visual interstellar extinction. The spectrum of the C-H stretch region of this object can be found in Figure 1a and its baseline corrected absorbance spectrum in Figure 5a.

### 3.4. VI Cygni # 12

The hypergiant Cygnus OB 2 no. 12 (VI Cygni # 12), classified as B5Ia<sup>+</sup>, is one of the most luminous stars in the Galaxy (Humphreys 1978). Because of its brightness and its large reddening ( $A_v \approx 10$  mag), it has often been used to study the infrared extinction law (Rieke 1974; Gillett et al. 1975; Roche & Aitken 1984a; Adamson et al. 1990). An absorption feature has been reported for this object at  $2950 \text{ cm}^{-1}$  ( $3.4 \mu\text{m}$ ) (Adamson et al. 1990) and is confirmed by our higher S/N data. This blue hypergiant is surrounded by a fast ( $\approx 1400 \text{ km s}^{-1}$ ), ionized wind ( $\dot{M} \approx 4 \times 10^{-5} M_\odot \text{ yr}^{-1}$ ; White & Becker 1983), which will have removed any circumstellar dust that might have formed during a previous evolutionary phase. Indeed, there is no evidence for associated infrared emission due to warm dust in the *IRAS* data base. All the extinction is therefore of interstellar origin. However, since this star is located at a distance of only 1.7 kpc (Torres-Dodgen, Tapia, & Carroll 1991) and the average visual extinction of the diffuse interstellar medium is  $\approx 2$  mag per kpc, it follows that most of this extinction is due to one (or a few) clouds along the line of sight. As indicated by the large variations of the visual extinction of other cluster members of the Cyg OB 2 association, this extinction is probably associated with local intercluster material, possibly the remnants of the parental cloud from which this association formed (Schulte 1958), and which is now being dispersed into the diffuse ISM.

Examination of our spectrum from this object (Fig. 1a) clearly shows that the use of linear baselines greatly overestimates the strength of the O-H and C-H features. Thus, we considered an additional case in which the continuum was represented by a baseline of the form  $A10^{Bv}$  where the constants were determined from least-squared fits to the entire data set to have values of  $A = 3.53 \times 10^{-13} \text{ watts m}^{-2} \mu\text{m}^{-1}$  and  $B = 4.523 \times 10^{-4} \text{ cm}$ . Comparison of the absorbance spectra obtained with these different baselines demonstrated that the general shape of the C-H feature was not greatly affected by the choice of baseline (a conclusion similar to that drawn by Adamson, Whittet, & Duley 1990), but that the linear continuum results in an inferred C-H band depth that is almost a factor of 2 larger. The exponential continuum clearly provided a better overall fit to the baseline and it was used to derive the absorbance plots shown in Figures 4 and 5a.

### 3.5. Ve 2–45 and AFGL 2179

The objects Ve 2–45 and AFGL 2179 are two examples of Population I, C-rich, Wolf-Rayet stars. They are massive WC 9 stars ( $> 20 M_\odot$ ) which, because of mass loss and mixing, show the products of nucleosynthesis in their photosphere (Abbott & Conti 1987). The spectra of WC stars show evidence for He, C, and O—approximately in the ratio 10:3:1 by number—but no evidence for H or N ( $< 10^{-2}$  and  $10^{-3}$  by number relative to He; Willis 1982; Nugis 1982; Torres 1988). Ve 2–45 and AFGL 2179 produce large excesses of infrared emission, presumably due to newly formed circumstellar carbon grains

(Williams, van der Hucht & Thé 1987). Recently, the identification with carbonaceous grains or molecules was placed on a firmer footing by the detection of a (weak)  $1300 \text{ cm}^{-1}$  ( $7.7 \mu\text{m}$ ) emission feature in the spectrum of Ve 2–45 (and in that of another WC 9 star, AFGL 2104; Cohen, Tielens, & Bregman 1989) thought to be due to carbon-carbon stretching vibrations in aromatic molecules. The total visual extinction towards Ve 2–45 and AFGL 2179 are estimated to be 6.5 and 12.8 mag, respectively, but the circumstellar shells contribute less than 0.5 mag (Cohen & Vogel 1978).

Our spectra of both these WC 9 sources are shown in Figure 1a. Broad band data show that background flux curves of both objects peak near  $3300 \text{ cm}^{-1}$  ( $3 \mu\text{m}$ ) and that the local continuum across the C-H feature can be well approximated by a linear baseline (Williams et al. 1987). The baseline corrected absorbance plots for these two objects can be found in Figure 5a. Given the absence of photospheric H in these objects, the circumstellar carbon grains associated with these objects are not expected to produce strong features due to C-H stretching vibrations. Thus, the extinction features seen in the absorbance plots for these objects in Figure 5a have an interstellar origin.

### 3.6. VI Cygni IRS 7

This bright infrared source lies in the general confines of the Cygnus OB 2 association and shows excess emission at wavelengths greater than  $2 \mu\text{m}$  (Ackermann 1970; Tapia 1981). This object has no known optical counterpart and its spectral class has not been determined. If it is a cluster member then its position within the cluster suggests a visual interstellar extinction of about 6 mag (Schulte 1958). The spectrum of this object is presented in Figure 1b and a baseline-corrected absorbance plot can be found in Figure 5b.

### 3.7. OH 01–477

OH 01–477 is an infrared source which is totally obscured at visual wavelengths and coincident with an OH source (Wickramasinghe & Allen 1980). This source appears to be a heavily obscured ( $A_v = 19$  mag) M4III star with a weak [ $A_v/\tau_{(3.4)} = 330 \pm 30$ ] feature near  $3.4 \mu\text{m}$  (Wickramasinghe & Allen 1980; Jones et al. 1982). This object was chosen for observation because its line of sight is very similar to that of the Galactic center sources. However, a considerable fraction of the visual extinction of this object might be circumstellar, rather than interstellar. The low- and high-resolution spectra of this object can be found in Figures 1b and 2, respectively. Baseline-corrected absorbance plots made from these spectra are presented in Figures 4 and 5b.

### 3.8. T629–5

T629–5 is an infrared source discovered by Tapia (1981). It is a very late Mira-type, M8III star reddened by  $A_v \approx 22$  as revealed by its near infrared spectrum and HKL photometry. The fraction of the extinction which is interstellar, as opposed to circumstellar, is not presently known. An earlier  $3300\text{--}2450 \text{ cm}^{-1}$  ( $3.0\text{--}4.1 \mu\text{m}$ ) spectrum of this object (Tapia et al. 1989) showed a broad absorption at  $\nu > 2700 \text{ cm}^{-1}$  ( $\lambda < 3.7 \mu\text{m}$ ), but the spectral resolution and signal-to-noise of the data were insufficient to determine whether O-H or C-H absorptions due to interstellar material were present. Our new low- and high-resolution spectra of this object can be found in Figures 1b and 2, respectively. Baseline-corrected absorbance plots made from these spectra are presented in Figures 4 and 5b.

## 3.9. OH 32.8–0.4

This object is a well-known OH maser source. OH phase lag measurements place it at distance of about 8 Kpc (Herman et al. 1984). Its spectral type is not known although its inferred luminosity suggests that it is a supergiant similar to VY CMA. Its infrared spectrum shows a deep silicate absorption feature near  $1000\text{ cm}^{-1}$  ( $10\text{ }\mu\text{m}$ ) and possibly an ice feature near  $3250\text{ cm}^{-1}$  ( $3.08\text{ }\mu\text{m}$ ) (Roche & Aitken 1984*b*). Because of the circumstellar emission and absorption, no reliable estimate of its interstellar extinction is available. Our spectrum of this object can be found in Figure 1*c*. This spectrum has been plotted on a log scale because of the great depth of the feature near  $3250\text{ cm}^{-1}$ . We do not detect the C-H stretch feature in the spectrum of this object and put an upper limit on its strength of  $\sim 1\%$ .

## 4. DISCUSSION

4.1. Absorption Features in the  $3600\text{--}2700\text{ cm}^{-1}$  ( $2.75\text{--}3.70\text{ }\mu\text{m}$ ) Region

A number of molecular vibrations can produce absorption features in the  $3600\text{--}2700\text{ cm}^{-1}$  ( $2.78\text{--}3.70\text{ }\mu\text{m}$ ) region. Considering only the most abundant elements, these include the O-H, N-H, and C-H stretching vibrations, and it is from amongst these that we are likely to find the source(s) contributing to the spectral structure evident in Figures 1 through 5. In H-bonded compounds, a broad ( $\Delta\nu \approx 300\text{ cm}^{-1}$ ) O-H stretch feature generally dominates the spectrum at frequencies above  $3000\text{ cm}^{-1}$  ( $3.3\text{ }\mu\text{m}$ ). Narrower ( $\Delta\nu \approx 10\text{--}50\text{ cm}^{-1}$ ) absorptions due to olefinic ( $=\text{C-H}$ ;  $\nu \geq 3000\text{ cm}^{-1}$ ) and acetylenic ( $\equiv\text{C-H}$ ;  $\nu \approx 3300 \pm 30\text{ cm}^{-1}$ ) C-H stretching vibrations, and N-H ( $\nu = 3400\text{--}3030\text{ cm}^{-1}$ ) stretching vibrations also fall in this region. Bands below  $3000\text{ cm}^{-1}$  most likely arise from the C-H stretch in aliphatic hydrocarbons. The C-H stretch in  $\text{CH}_4$  and aromatic hydrocarbons generally fall within  $50\text{ cm}^{-1}$  of  $3000\text{ cm}^{-1}$  ( $3.3\text{ }\mu\text{m}$ ).

Many of our spectra show broad absorption features centered near  $3300$  and/or  $2950\text{ cm}^{-1}$  ( $3.0$  and  $3.4\text{ }\mu\text{m}$ ). In line with the preceding discussion, the former is attributed to O-H stretching vibrations and the latter to C-H stretching vibrations in aliphatic  $-\text{CH}_2-$  and  $-\text{CH}_3$  groups. Analysis of the spectra indicate that these features have several different origins. For instance, we will show that absorption in the  $3.4\text{ }\mu\text{m}$  spectral region of some sources is due to photospheric material, while in other sources it is associated with material in the diffuse ISM.

4.1.1. The O-H/C-H Ratio and the Origin of the Bands near  $3300$  and  $2950\text{ cm}^{-1}$  ( $3.0$  and  $3.4\text{ }\mu\text{m}$ )

The infrared absorption features near  $3300$  and  $2950\text{ cm}^{-1}$  ( $3.0$  and  $3.4\text{ }\mu\text{m}$ ) generally associated with the diffuse medium were first studied by Soifer et al. (1976) and Wickramasinghe & Allen (1980) when they examined the Galactic center source IRS 7. This object has been the focus of a number of subsequent studies since it is bright in the infrared and its interstellar extinction is probably dominated by material in the diffuse interstellar medium, although there may be some contribution from molecular cloud material (Allen & Wickramasinghe 1981; Jones, Hyland, & Allen 1983; Willner & Pipher 1982; Butchart et al. 1986; McFadzean et al. 1989). The  $3300\text{ cm}^{-1}$  peak is generally ascribed to O-H stretching vibrations and the  $2950\text{ cm}^{-1}$  feature to C-H stretching vibrations (Wickramasinghe & Allen 1980; Allamandola 1984; Butchart et al. 1986; McFadzean et al. 1989).

Critical questions raised by the spectrum of GC IRS 7 concern the origins of the O-H and C-H bands, especially in light of the wide variations in the spectra of the other Galactic center sources studied by Willner & Pipher (1982). This question was critically considered by McFadzean et al. (1989) in their recent study of several Galactic center sources. They concluded that the O-H arises from material local to the Galactic center whereas the C-H feature is produced by material in the diffuse interstellar medium. We too have investigated this question, not by focusing on multiple sources along the line of sight to the Galactic center, but on sources thought to suffer extinction by dust in the diffuse medium which lie along several very different directions in the Galactic plane. It is clear from the variations between the depth of the O-H band near  $3300\text{ cm}^{-1}$  ( $3.0\text{ }\mu\text{m}$ ) and the depth of the C-H band near  $2950\text{ cm}^{-1}$  ( $3.4\text{ }\mu\text{m}$ ) that these features do not originate from the same carrier (Fig. 4). In particular, note that while the  $\tau_{\text{OH}}/\tau_{\text{CH}}$  ratio is less than 0.25 for VI Cygni #12, it is about 4 for GC IRS 7. However, even if the materials that produce the O-H and C-H features are independent, it is still possible that both reside in the diffuse interstellar medium. The absence of clear absorption attributable to any O-H stretch towards VI Cygni #12 indicates that the dust in the diffuse medium toward this object does not contain significant amounts of O-H, either as part of the hydrocarbon molecules which produce the C-H feature (i.e., it is not due to O-H in alcohols, glycerols, or phenols), or as  $\text{H}_2\text{O}$  molecules trapped in a H-bonded material.

## 4.1.2. Features with Origins in the Diffuse Interstellar Medium—The C-H Stretch Region

Comparison of the spectra in Figures 5*a* and 5*b* shows that there is a strong similarity between the C-H absorption features towards VI Cygni #12, GC IRS 7, GC IRS 3, Ve 2–45, and AFGL 2179, and that these features are distinctly different from those of OH 01–477 and T629–5. The remarkable match of the C-H features of VI Cygni #12 and GC IRS 7 can be seen in Figure 6 where we have plotted the absorbance spectrum of GC IRS 7 and the scaled absorbance spectrum of VI Cygni #12. This suggests that the feature in these two objects is largely due to material in the diffuse interstellar medium. Likewise, the C-H stretch features we observe at low resolution towards GC IRS 3 and the two WC stars Ve 2–45 and AFGL 2179 are quite similar to the low-resolution spectrum of GC IRS 7. In addition, as we will demonstrate later in the paper, the strength of these features correlates well with the amount of visual extinction towards these objects. Thus, we attribute the origin of the C-H absorption in the spectra of VI Cygni #12, GC IRS 7, GC IRS 3, Ve 2–45, and AFGL 2179 to carbonaceous material in the diffuse interstellar medium.

## 4.1.3. Features with Origins in Circumstellar, Photospheric, or Dense Cloud Materials

*The O-H Stretch Region.* Figure 4 illustrates that the profile of the broad O-H stretching band, which extends from about  $3450$  to  $3100\text{ cm}^{-1}$  ( $2.90\text{--}3.23\text{ }\mu\text{m}$ ) in our spectra, is similar in OH 01–477, T629–5, and GC IRS 7. The O-H band might be fit by laboratory spectra of ices of  $\text{H}_2\text{O}$  and alcohols (Schutte 1988) and by “water of hydration” in silicates (Sandford & Walker 1985). Other possible interstellar materials that might contribute at these frequencies include N-H bearing compounds, olefins, and acetylenes. In the case of GC IRS 7, McFadzean et al. (1989) have suggested that the O-H band originates from a local molecular cloud. Our observations pre-

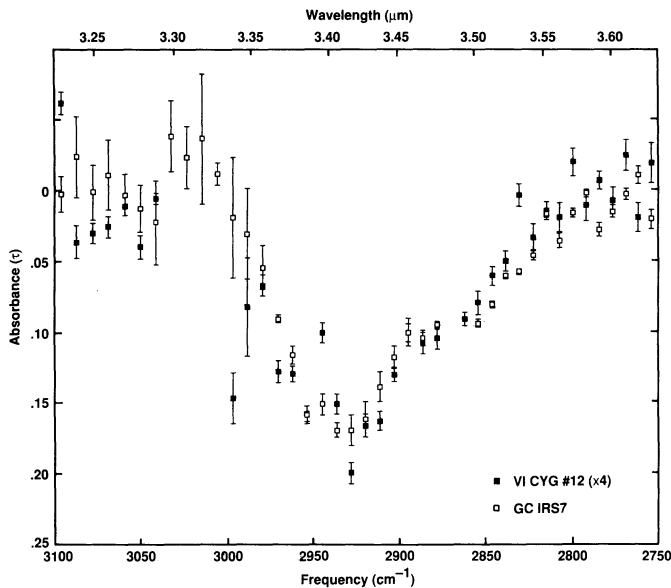


FIG. 6.—A comparison between the profile of the C-H stretching feature (in absorbance) in the spectra of GC IRS 7 and VI Cygni #12. The optical depth values in the VI Cygni #12 spectrum have been scaled by a factor of 4. Both spectra were taken at a resolution of  $0.018 \mu\text{m}$  per detector and double-sampled with a  $\frac{1}{2}$  channel shift.

sently cannot determine whether the O-H feature is derived from diffuse material, or results from more localized sources.

The spectrum of OH 32.8–0.3 (Fig. 1c) in the O-H stretching region is probably dominated by circumstellar material. This is suggested by the deep silicate absorption feature near  $1000 \text{ cm}^{-1}$  ( $10 \mu\text{m}$ ) and probable  $\text{H}_2\text{O}$  ice feature near  $3250 \text{ cm}^{-1}$  ( $3.08 \mu\text{m}$ ) seen in the spectra of this object (Roche & Aitken 1984b, and data presented here).

*The C-H Stretch Region.* Comparison of the strengths of the C-H features attributed to diffuse medium dust towards VI Cygni #12 and GC IRS 7 with the visual extinctions towards these two objects suggests that we should have detected this feature in the spectra of VI Cygni IRS 7, T629–5, and OH 01–477 if all of their extinction has an interstellar origin. However, it is apparent from Figures 2 and 5a that the high-resolution spectra of T629–5 and OH 01–477 are distinctly different from that of GC IRS 7.

The spectra of T629–5 and OH 01–477 are dominated by a series of narrow bands separated by a fairly regular spacing of about  $50 \text{ cm}^{-1}$  (see Table 2). Both T629–5 and OH 01–477 are M stars. M stars often show spectral structure due to photospheric materials (see Ridgeway 1984). Comparison of the features seen in the high resolution spectra of T629–5 and OH 01–477 with the reported positions of the strongest photospheric OH bands seen in the spectrum of the M supergiant  $\alpha$  Orionis (Beer et al. 1972) strongly suggests that photospheric OH is responsible for much of the observed spectral structure (Table 2). Preliminary reduction of subsequent high- and low-resolution CGAS spectra measured from the unobscured M stars V842 Aql (M6+III:) and ST Cep (M2 Ia-Iab) on 1990 July 26–27 from the IRTF show good correspondence with the OH features listed in Table 2. Thus, while it is possible that dust in the diffuse medium is contributing to the absorption in this spectral region towards T629–5 and OH 01–477, we are presently unable to quantitatively separate the inter-

TABLE 2

COMPARISON OF BAND POSITIONS IN THE  $3200\text{--}2700 \text{ cm}^{-1}$  ( $3.1\text{--}3.7 \mu\text{m}$ ) SPECTRAL REGION WITH KNOWN PHOTOSPHERIC OH FEATURES

OH 01–477 ( $\text{cm}^{-1}$ )	T629–5 ( $\text{cm}^{-1}$ )	VI Cygni IRS 7 ( $\text{cm}^{-1}$ )	Possible Band Assignments <sup>a</sup>
...	...	$\sim 2750$	OH 2-1 K = 15 and OH 3-2 K = 12
...	...	$\sim 2790$	OH 1-0 K = 17
2838 (s)	2840 (s)	$\sim 2840$	OH 1-0 K = 16
...	2860 (m)	...	ISM?
2870 (w)	...	...	ISM?
2890 (s)	2890 (s)	$\sim 2890$ (?)	OH 1-0 K = 15
2940 (s)	2940 (s)	$\sim 2940$	OH 1-0 K = 14 and OH 2-1 K = 11
2995 (?) (s)	2990 (s)	$\sim 2990$	OH 1-0 K = 13 and OH 2-1 K = 10
...	3045 (s)	$\sim 3040$	OH 1-0 K = 12 and OH 2-1 K = 9
...	3080 (?) (s)	$\sim 3080$	OH 2-1 K = 8

NOTE.—Features measured from Fig. 5b; s, m, and w represent band strengths which are strong, moderate, or weak, respectively.

<sup>a</sup> Identifications made from Beer et al. 1972.

stellar contribution from the photospheric OH features due to the greater strengths of the latter.

This raises the question as to why these features are not evident in the spectra of GC IRS 7 or GC IRS 3, as both are thought to be M stars as well. Close inspection of the high-resolution spectrum of GC IRS 7 (Figures 2 and 5a) shows that there may be evidence for sharp, weak components at about 2995, 2945, 2895, and perhaps  $2840 \text{ cm}^{-1}$  ( $3.339$ ,  $3.396$ ,  $3.454$ , and  $3.521 \mu\text{m}$ ), superposed on the broad absorption feature. These bands match the positions of the strongest lines in the spectra of T629–5 and OH 01–477 and may arise from photospheric OH. Thus, caution is warranted in attributing all the absorption in these objects to interstellar dust.

The regular spacing and position of the features in the low-resolution spectrum of VI Cygni IRS 7 is also suggestive of the presence of OH (Table 2). However, the photometric colors of VI Cygni IRS 7 are not compatible with the source being an M star (Torres-Dodgen et al. 1991). Final identification of the spectral structure produced by this object will have to wait for additional, higher resolution data.

#### 4.2. The Hydrocarbon Component of Dust in the Diffuse Interstellar Medium

##### 4.2.1. Chemical Composition

The profile and subpeak positions of the C-H stretching features in Figure 5a provide specific clues to the nature of the carbonaceous material in the diffuse interstellar medium. The hydrocarbon feature in the low-resolution spectra extends from about  $2800 \text{ cm}^{-1}$  ( $3.57 \mu\text{m}$ ) to  $3000 \text{ cm}^{-1}$  ( $3.33 \mu\text{m}$ ) with suggestions of subpeaks at about  $2955$  and  $2930 \text{ cm}^{-1}$  ( $3.38$  and  $3.41 \mu\text{m}$ ) and a broad shoulder near  $2860 \text{ cm}^{-1}$ . The exact position of the center of the shoulder is uncertain because the CGAS detector at this position is unreliable. The higher resolution spectrum of GC IRS 7 shows subfeatures at  $2957$ ,  $2926$ , and  $2870 \text{ cm}^{-1}$  ( $3.38$ ,  $3.42$ , and  $3.48 \mu\text{m}$ ; excluding the possible features associated with M stars). *These peak positions closely match, to within  $5 \text{ cm}^{-1}$  (better than 1 part in 500), the symmetric and asymmetric C-H stretching frequencies of  $-\text{CH}_3$  (methyl) and  $-\text{CH}_2-$  (methylene) groups in saturated aliphatic hydrocarbons (Table 3). The general formula for saturated,*

TABLE 3  
COMPARISON OF THE C-H STRETCHING BAND FREQUENCIES ( $\text{cm}^{-1}$ ) IN THE SPECTRA OF GC IRS 7 WITH THOSE OF SEVERAL TYPES OF HYDROCARBONS AT 10 K

VIBRATION	GC IRS 7	FREQUENCY ( $\text{cm}^{-1}$ ) <sup>a</sup>								
		SATURATED ALIPHATICS Pentane ( $\text{C}_5\text{H}_{12}$ )	Hexane ( $\text{C}_6\text{H}_{14}$ )	Cyclohexane ( $\text{C}_6\text{H}_{12}$ )	Methyl Cyclohexane ( $\text{C}_7\text{H}_{14}$ )	ALIPHATICS WITH ELECTRONEGATIVE GROUPS Butanol ( $\text{C}_4\text{H}_9\text{OH}$ )	Methanol ( $\text{CH}_3\text{OH}$ )	Methylcyanide ( $\text{CH}_3\text{CN}$ )	Formaldehyde <sup>b</sup> ( $\text{H}_2\text{CO}$ , pure)	Formaldehyde <sup>b</sup> ( $\text{H}_2\text{CO}$ , in $\text{H}_2\text{O}$ )
$-\text{CH}_3$ Asymmetric	2957	2957	2955	...	2946	2955	2982	3001	...	...
C-H Stretch	2926	2923	2921	2927	2926 (2908)	2928	2950	...	2886	2853
$-\text{CH}_2-$ Asymmetric	2870	2872	2870	...	2868	2869	2828	2941	...	...
C-H Stretch	...	2857	2858	2850	2850	...	...	...	2823	2785

<sup>a</sup> GC IRS 7 frequencies are accurate to within  $5 \text{ cm}^{-1}$ ; laboratory frequencies to within  $2 \text{ cm}^{-1}$ . Band positions for the chemical standards are from d'Hendecourt & Allamandola 1986.

<sup>b</sup> From van der Zwet et al. 1985; other aldehydes often have 2 bands in the  $2830\text{--}2695 \text{ cm}^{-1}$  ( $3.53\text{--}3.71 \mu\text{m}$ ) region (Silverstein & Bassler 1967).

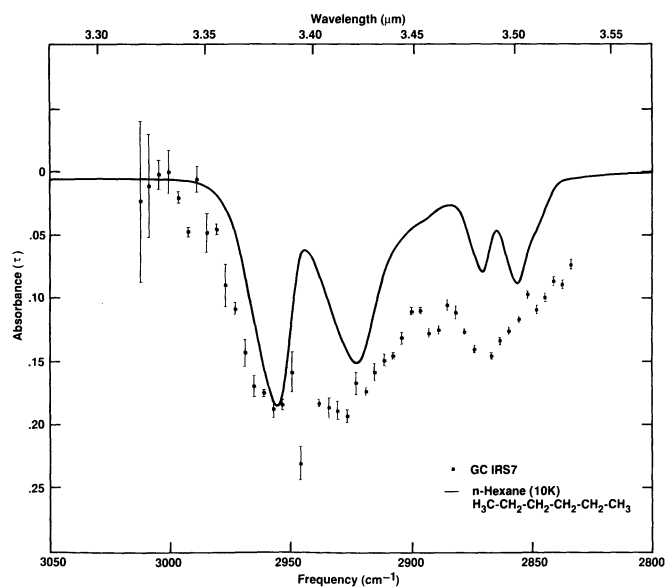


FIG. 7a

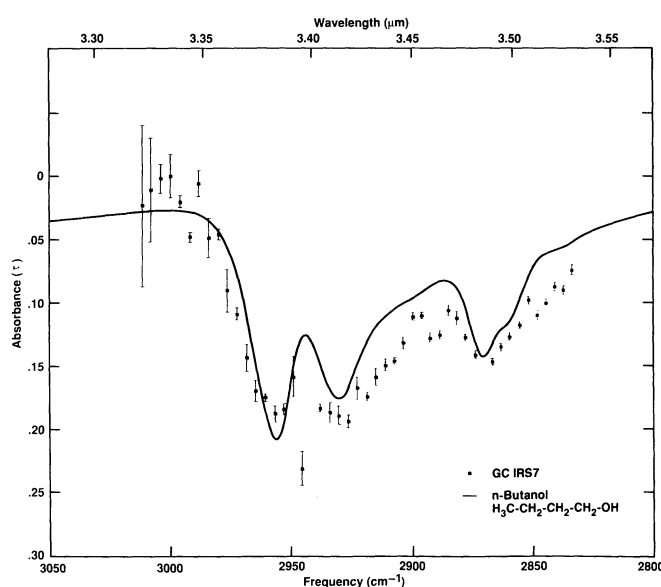


FIG. 7b

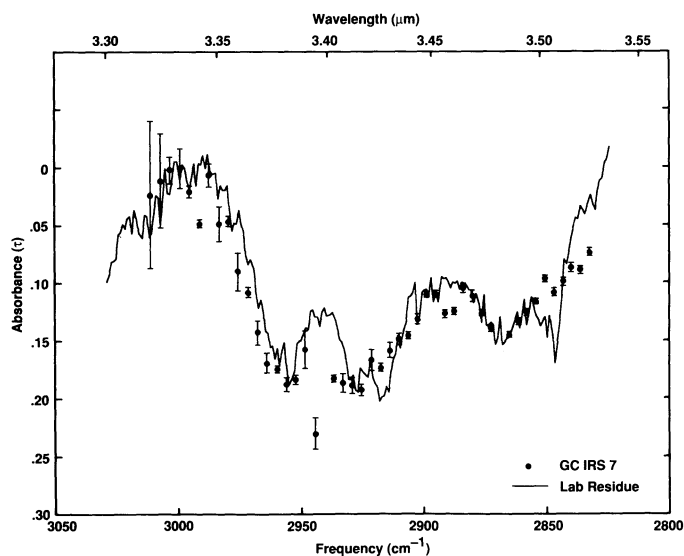


FIG. 7c

FIG. 7.—(a) Comparison between the profile of the C-H stretching feature in absorbance seen towards GC IRS 7 (points) and the C-H stretching feature of the saturated aliphatic hydrocarbon hexane (C<sub>6</sub>H<sub>14</sub>) at 10 K. The spectral data from GC IRS 7 have a resolution of 0.004 μm per detector. The lab spectrum has a resolution of 1 cm<sup>-1</sup>. (b) Comparison between the profile of the C-H stretching feature in absorbance seen towards GC IRS 7 (points) and the C-H stretching feature of the alcohol butanol (C<sub>4</sub>H<sub>9</sub>OH) at 10 K. In *n*-butanol, one of the -CH<sub>2</sub>-CH<sub>3</sub> ends of *n*-hexane (Fig. 7a) has been replaced by an electronegative -O-H group. The spectra have the same resolutions as in Fig. 7a. (c) Comparison between the profile of the C-H stretching feature in absorbance seen towards GC IRS 7 (points) and the C-H stretching feature measured from a laboratory residue. The laboratory residue was produced by depositing an H<sub>2</sub>O:CH<sub>3</sub>OH:NH<sub>3</sub>:CO:C<sub>3</sub>H<sub>8</sub> = 10:5:1:1:1 ice at 10 K, irradiating it with ultraviolet photons, and warming it to 200 K (Allamandola, Sandford, & Valero 1988). The residue that remains provides a good fit to the GC IRS 7 spectrum in the C-H stretch region except where the source shows additional absorption features thought to arise from photospheric OH (see text). The spectra have the same resolutions as in Fig. 7a.

unbranched hydrocarbons is CH<sub>3</sub>-(CH<sub>2</sub>)<sub>*n*</sub>-CH<sub>3</sub>. For *n* up to about 10, these molecules are gases or clear liquids (i.e., propane, *n* = 3; butane, *n* = 4; hexane, *n* = 6; octane, *n* = 8), while molecules with increasingly larger values of *n* become oils and then waxes (such as in paraffin and candles). The very close match in peak position of these three bands to those in saturated aliphatics (see pentane and hexane in Table 3) implies that electronegative groups such as aromatic rings, hydroxy (-O-H) or cyano (-C≡N) are not chemically bonded adjacent to the C-H bonds responsible for these bands. The nearby presence of these other chemical groups would shift the positions of the C-H bands from their nominal interstellar positions (see methanol and methyl-cyanide in Table 3). However, the interstellar band profile differs from that of saturated aliphatic hydrocarbons in that it does not show a clear peak near 2855 cm<sup>-1</sup> (3.503 μm) (see Figure 7a). The presence

of minor amounts of electronegative groups can strongly suppress this feature in aliphatic chains without greatly affecting the positions of the other three bands. For example, Figure 7b shows a comparison between the spectrum of GC IRS 7 and the spectrum of solid *n*-butanol (Table 3), an alcohol in which one of the -CH<sub>2</sub>-CH<sub>3</sub> ends of *n*-hexane (Figure 7a) has been replaced by an electronegative -O-H group. The presence of a different group perturbs the local force fields within the molecule and affects the bond force constants, causing band shifts and broadening. The effect of the electronegative group diminishes with distance and only the closest aliphatic groups are influenced. Thus, -CH<sub>2</sub>- and -CH<sub>3</sub> groups that are separated from the electronegative group by several intermediate carbon atoms will produce essentially aliphatic spectral features. A similar effect is expected for molecules in which the -O-H group is replaced by other electronegative groups. The

TABLE 4  
SPECTROSCOPIC PROPERTIES OF THE C-H STRETCHING FUNDAMENTALS OF SATURATED ALIPHATIC  
HYDROCARBONS AT 10 K<sup>a</sup>

Vibrational Mode	C <sub>3</sub> H <sub>12</sub> H <sub>3</sub> C-(CH <sub>2</sub> ) <sub>3</sub> -CH <sub>3</sub>	C <sub>6</sub> H <sub>14</sub> H <sub>3</sub> C-(CH <sub>2</sub> ) <sub>4</sub> -CH <sub>3</sub>	Cyclo-C <sub>6</sub> H <sub>12</sub> Cyclo-(CH <sub>2</sub> ) <sub>6</sub>	Average Values <sup>b</sup>
-CH <sub>3</sub> Asymmetric Stretch				
$\nu$ (cm <sup>-1</sup> )	2957	2955	...	2955
$\Delta\nu$ (cm <sup>-1</sup> )	17	18	...	18
$A$ /molecule (cm molecule <sup>-1</sup> )	$2.3 \times 10^{-17}$	$2.2 \times 10^{-17}$	...	$2.3 \times 10^{-17}$
$A$ /CH <sub>3</sub> (cm group <sup>-1</sup> )	$1.2 \times 10^{-17}$	$1.1 \times 10^{-17}$	...	$1.2 \times 10^{-17}$
-CH <sub>2</sub> - Asymmetric Stretch				
$\nu$ (cm <sup>-1</sup> )	2923	2921	2927	2925
$\Delta\nu$ (cm <sup>-1</sup> )	20	28	17	22
$A$ /molecule (cm molecule <sup>-1</sup> )	$2.4 \times 10^{-17}$	$2.2 \times 10^{-17}$	$5.3 \times 10^{-17}$	$3.3 \times 10^{-17}$
$A$ /CH <sub>2</sub> (cm group <sup>-1</sup> )	$8 \times 10^{-18}$	$5.5 \times 10^{-18}$	$8.8 \times 10^{-18}$	$7.4 \times 10^{-18}$
-CH <sub>3</sub> Symmetric Stretch				
$\nu$ (cm <sup>-1</sup> )	2872	2870	...	2870
$\Delta\nu$ (cm <sup>-1</sup> )	9	10	...	10
$A$ /molecule (cm molecule <sup>-1</sup> )	$4.8 \times 10^{-18}$	$3.6 \times 10^{-18}$	...	$4.2 \times 10^{-18}$
$A$ /CH <sub>3</sub> (cm group <sup>-1</sup> )	$2.4 \times 10^{-18}$	$1.8 \times 10^{-18}$	...	$2.1 \times 10^{-18}$
-CH <sub>2</sub> - Asymmetric Stretch				
$\nu$ (cm <sup>-1</sup> )	2857	2858	2850	2855
$\Delta\nu$ (cm <sup>-1</sup> )	14	10	11	12
$A$ /molecule (cm molecule <sup>-1</sup> )	$9 \times 10^{-18}$	$3.6 \times 10^{-18}$	$1.4 \times 10^{-17}$	$8.9 \times 10^{-18}$
$A$ /CH <sub>2</sub> (cm group <sup>-1</sup> )	$3 \times 10^{-18}$	$9 \times 10^{-19}$	$2.3 \times 10^{-18}$	$2.1 \times 10^{-18}$

<sup>a</sup> Data from d'Hendecourt & Allamandola (1986).

<sup>b</sup> Frequencies listed are rounded to the nearest 5 cm<sup>-1</sup>.

improvement in match to the astronomical data from Figure 7a to Figure 7b strongly supports the suggestion that the C-H stretch feature produced by interstellar dust is largely due to short ( $n = 2-4$ ) aliphatic chains that either contain, or are attached to, electronegative groups like -O-H and -C≡N.

In view of the good peak position match of the interstellar bands near 2957 and 2926 cm<sup>-1</sup> to those of saturated aliphatic hydrocarbons, the spectroscopic properties of these organic compounds, summarized in Table 4, can be used to quantitatively analyze the interstellar features. The column density,  $N$  (molecules cm<sup>-2</sup>) of material producing an infrared absorption can be determined from

$$N = \frac{\tau \Delta\nu}{A} \quad (1)$$

where  $\tau$  is the optical depth (absorbance);  $\Delta\nu$  is the full-width-at-half-maximum (cm<sup>-1</sup>) for absorbance spectra; and  $A$  is the integrated absorbance in cm molecule<sup>-1</sup> (e.g., d'Hendecourt & Allamandola 1986). We have used equation (1) to calculate the values of  $N$  that correspond to the  $\tau$  values for the 2955 and 2925 cm<sup>-1</sup> asymmetric C-H stretching bands in the spectra shown in Figure 5a. Corresponding calculations were not made using the 2870 and 2850 cm<sup>-1</sup> symmetric C-H stretching bands for two reasons. First, in our low-resolution data this spectral region was covered by a detector that was not operating reliably during these observations. Second, the spectra do not extend to sufficiently low frequencies to establish the continuum as accurately as can be done for the higher frequency peaks. The column densities for the -CH<sub>2</sub>- and -CH<sub>3</sub> groups are summarized in Table 5 and were derived using the  $A$  and  $\Delta\nu$  values from Table 4 and the  $\tau$  values given in Table 5.

An important conclusion concerning the composition of the dust can be drawn from the column densities of the asymmetric stretching bands listed in Table 5. The average -CH<sub>2</sub>-/-CH<sub>3</sub>

TABLE 5  
OPTICAL DEPTH, COLUMN DENSITIES OF THE METHYL (-CH<sub>3</sub>) AND  
METHYLENE (-CH<sub>2</sub>) DIFFUSE INTERSTELLAR MEDIUM DUST  
COMPONENTS AND RELATION TO  $A_v$ <sup>a</sup>

Object <sup>b</sup>	Parameters	-CH <sub>3</sub> (2955 cm <sup>-1</sup> )	-CH <sub>2</sub> - (2925 cm <sup>-1</sup> )
VI Cygni #12 ( $A_v = 10$ )	$\nu$	2952	2927
	$\tau$	0.04	0.05
	$N$	$5.9 \times 10^{16}$	$1.5 \times 10^{17}$
	$A_v/\tau$	255	200
AFGL 2179 ( $A_v = 12.8$ )	$\nu$	2952	2919
	$\tau$	0.03	0.05
	$N$	$4.7 \times 10^{16}$	$1.4 \times 10^{17}$
	$A_v/\tau$	405	280
Ve 2-45 ( $A_v = 6.5$ )	$\nu$	2952	2919
	$\tau$	0.02	0.02
	$N$	$2.8 \times 10^{16}$	$7.3 \times 10^{16}$
	$A_v/\tau$	345	265
GC IRS 7 ( $A_v = 31$ ) (low resolution)	$\nu$	2953	2937
	$\tau$	0.16	0.17
	$N$	$2.4 \times 10^{17}$	$5.0 \times 10^{17}$
	$A_v/\tau$	215	200
GC IRS 7 ( $A_v = 31$ ) (high resolution)	$\nu$	2957	2926
	$\tau$	0.19	0.19
	$N$	$2.8 \times 10^{17}$	$5.7 \times 10^{17}$
	$A_v/\tau$	180	175
GC IRS 3 ( $A_v = 31$ )	$\nu$	2952	2919
	$\tau$	0.25	0.24
	$N$	$3.8 \times 10^{17}$	$7.3 \times 10^{17}$
	$A_v/\tau$	120	125

<sup>a</sup> Units are:  $\nu$  (cm<sup>-1</sup>);  $N$  (groups/cm<sup>2</sup>); band positions are accurate to 5 cm<sup>-1</sup>; the uncertainty in the stated  $\tau$  values is on the order of 20%-30% and is dominated by uncertainties in the baselines underlying the features (see text).

<sup>b</sup> Listed  $A_v$  values represent best estimates of the extinction due to diffuse interstellar material only.

ratio of the interstellar hydrocarbon is  $2.5 \pm 0.4$ . This suggests that the hydrocarbon grain material in the diffuse medium may consist of a mixture of cross-linked hydrocarbon molecules containing structures like  $-\text{CH}_2-\text{CH}_2-\text{CH}_3$  and  $-\text{CH}_2-\text{CH}_2-\text{CH}_2-\text{CH}_3$ . Note that the  $-\text{CH}_2-/-\text{CH}_3$  ratio is 2.0 for the hexane whose spectrum is shown in Figure 7a. This underabundance of  $-\text{CH}_2-$  groups is one of the reasons why the relative strengths of the subpeaks in the overall C-H stretch feature in Figure 7a do not match those in the GC IRS 7 spectrum.

At this point it is important to stress what these data do *not* tell us about the carbonaceous material in the diffuse interstellar medium. The C-H band only carries information about the  $\text{sp}^3$  carbon atoms to which hydrogen is attached. This band yields no information about those carbon atoms which are bonded to heavier elements or to the carbon atoms that make up the  $\text{sp}^2$  and  $\text{sp}^3$  bonded skeleton of amorphous carbon, alkenes, alkynes, and aromatic molecules.

#### 4.2.2. The Production of the C-H Band Carrier Via Ultraviolet Photolysis of Ices in Dense Molecular Clouds

We have been studying the UV photolysis of mixed-molecular interstellar ice analogs such as  $\text{H}_2\text{O}:\text{CH}_3\text{OH}:\text{NH}_3:\text{CO}$  (100:50:1:1) because their infrared spectra reproduce many of the major spectral features attributed to the ice component of dense molecular clouds (Tielens & Allamandola 1987; Allamandola, Sandford, & Valero 1988). In several of these experiments small amounts of simple saturated hydrocarbons such as propane ( $\text{C}_3\text{H}_8$ ) and hexane ( $\text{C}_6\text{H}_{14}$ ) were also included in the starting mixture. These mixtures were deposited under vacuum at low temperatures (typically 10 K), exposed to UV radiation for 1 to 40 hr, and then warmed to remove the more volatile components. At temperatures of 200 K and above, only complex, photoproduct residues remain on the substrate. The spectra of the residues from these various experiments are all quite similar and are relatively insensitive to the exact concentrations of the starting ices (Allamandola et al. 1988).

In order to make a direct comparison between the laboratory residue and the interstellar material, a flat baseline has been applied across the C-H stretch band of the residue spectra and absorbance (optical depth) plots prepared in the same manner as described in the Data and Results section. A comparison between the high resolution absorbance spectrum of GC IRS 7 and a representative residue produced by the UV irradiation of an  $\text{H}_2\text{O}:\text{CH}_3\text{OH}:\text{CO}:\text{NH}_3:\text{C}_3\text{H}_8$  (100:50:10:10:10) ice at 10 K, which was subsequently warmed to 200 K, is shown in Figure 7c. *The excellent agreement in feature profile and substructure between the two spectra*

*suggest that the material produced by the laboratory irradiation of these interstellar ice analogs is very similar in nature to the hydrocarbon component of the dust in the diffuse interstellar medium.* This is consistent with a model in which the hydrocarbon component we have observed in the diffuse interstellar medium is comprised in large part of a complex mixture of interlinked, aliphatic hydrocarbons produced in dense molecular clouds and subsequently modified in the diffuse ISM.

The fit of the interstellar C-H stretch feature with the aliphatic component in organic residues requires that spectral structure exist at lower frequencies, particularly in the 2000–1250  $\text{cm}^{-1}$  (5–8  $\mu\text{m}$ ) region (Allamandola et al. 1988). A preliminary comparison in the 2000–1250  $\text{cm}^{-1}$  region between the spectrum of GC IRS 7 and the laboratory spectrum that fits the C-H stretch feature reveals some striking similarities (Willner et al. 1979; Tielens et al. 1991).

#### 4.2.3. Relationships to Visual Extinction, Column Densities, and Abundances

The optical depth of the C-H stretch feature [ $\tau_{(\text{CH})}$ ] and  $A_v$  values listed in Table 5 can be used to derive important parameters associated with interstellar dust. First, absorption versus visual extinction relationships for the  $-\text{CH}_2-$  and  $-\text{CH}_3$  hydrocarbon components of the dust can be derived. Second, it is possible to determine the column densities of the  $-\text{CH}_3$  and  $-\text{CH}_2-$  groups. Finally, it is possible to place constraints on the fraction of the cosmic carbon along the line of sight that is tied up in these chemical groups.

The  $\tau_{(\text{CH})}$  and  $A_v$  values listed in Table 5 show that  $A_v/\tau_{(2925\text{ cm}^{-1})} = 240 \pm 40$  and  $A_v/\tau_{(2955\text{ cm}^{-1})} = 310 \pm 90$ . (The values for GC IRS 3 have been excluded from this calculation since there is the potential that a significant fraction of the observed absorption is contributed by photospheric OH. These values drop by 10–15% if GC IRS 3 is included.) This correlation along different lines of sight strongly suggests that the C-H feature arises from interstellar material. Detection of the C-H feature towards additional objects having different amounts of visual extinction will be needed to further refine this relationship.

The percentage of cosmic carbon tied up in the interstellar hydrocarbon component can be determined as follows. The column densities of hydrogen listed in Table 6 were derived using the standard relation

$$N_{\text{H}} = 1.9 \times 10^{21} A_v \quad (2)$$

given by Bohlin et al. (1978). The abundance of carbon,  $N_{\text{C}}$ , along these same lines of sight, also presented in Table 6, was then derived assuming a cosmic carbon to hydrogen ratio of  $3.7 \times 10^{-4}$  (Allen 1973). The corresponding column densities of  $-\text{CH}_3$  and  $-\text{CH}_2-$  groups,  $N_{\text{CH}_3}$  and  $N_{\text{CH}_2}$ , were then deter-

TABLE 6  
HYDROGEN, CARBON,  $-\text{CH}_3$  AND  $-\text{CH}_2-$  COLUMN DENSITIES AND THE PERCENT OF COSMIC CARBON  
IN THE ALIPHATIC HYDROCARBON COMPONENT OF DIFFUSE MEDIUM DUST

Object	$A_v$	$\tau_{(\text{sil})}$	$N(\text{H})$	$N(\text{C})$	$N(\text{CH}_3)$	$N(\text{CH}_2)$	%C <sup>a</sup>
VI Cygni # 12	10	$0.58 \pm 0.1$	$1.9 \times 10^{22}$	$7.0 \times 10^{18}$	$5.9 \times 10^{16}$	$1.5 \times 10^{17}$	3.0
AFGL 2179	12.8	...	$2.4 \times 10^{22}$	$9.0 \times 10^{18}$	$4.7 \times 10^{16}$	$1.4 \times 10^{17}$	2.1
Ve 2–45	6.5	...	$1.2 \times 10^{22}$	$4.6 \times 10^{18}$	$2.8 \times 10^{16}$	$7.3 \times 10^{16}$	2.2
GC IRS 7	34	$3.6 \pm 0.4$	$6.5 \times 10^{22}$	$2.4 \times 10^{19}$	$2.4 \times 10^{17}$	$5 \times 10^{17}$	3.1
GC IRS 3	30	...	$5.7 \times 10^{22}$	$2.1 \times 10^{19}$	$3.8 \times 10^{17}$	$7.3 \times 10^{17}$	5.2

<sup>a</sup> This is a lower limit for the percent of cosmic carbon which is tied up in the  $-\text{CH}_3$  and  $-\text{CH}_2-$  groups combined. The upper limit is about 10 times higher (see text).

mined using the  $\tau$  values from Table 5 and the integrated absorbance values,  $A$ , listed in Table 4. Averaging the values for the lines of sight we have studied, we find an absolute lower limit of  $2.6 \pm 0.5\%$  of cosmic carbon is tied up in the aliphatic component of the dust. This is a lower limit because the  $A$  values used were those appropriate for pure saturated aliphatic hydrocarbons (i.e., for  $-\text{CH}_2-$  and  $-\text{CH}_3$  groups that are not close to electronegative groups), and these  $A$  values are typically larger than those for the same vibrations in other hydrocarbons. When adjacent to an electronegative group, the  $A$  value per  $-\text{CH}_2-$  and  $-\text{CH}_3$  group can be as much as 10 times lower (although factors of 2–3 are more common). Thus, even if most of the  $-\text{CH}_2-$  and  $-\text{CH}_3$  groups in the interstellar material were adjacent to an electronegative group, the C-H stretching feature we observe would be dominated by the nonadjacent aliphatics. Considering the extreme case in which each interstellar aliphatic group is accompanied by 10 times as many like groups near electronegatives, one derives an upper limit of about 25% for the total carbon associated with material that produces the interstellar C-H feature. We remind the reader that this abundance range is based on absorbance (optical depth) plots that were derived using conservative baselines. Thus, the extreme upper limit could be as high as 35%. This limit can be considered an upper limit since the presence of this many electronegative groups in the interstellar material would produce a C-H feature very different from that measured from GC IRS 7. In view of the better match to the GC IRS 7 spectrum by the butyl group attached to -O-H (Figure 7b), intermediate  $A$  values are probably more appropriate for the overall interstellar C-H stretch feature. Using  $A$  values typical of short chain alcohols, we derive a value of  $\sim 10\%$  for the total carbon associated with the ISM material that produces the C-H stretch band. The complex laboratory hydrocarbons which reproduce the interstellar feature also have  $A$  values which are intermediate to those appropriate for aliphatic groups in pure saturated hydrocarbons and those close to electronegative groups. Thus, we conclude that the percentage of cosmic carbon producing the interstellar C-H stretch feature is about 10%. The range of 2.6%–35% encompasses the 10% estimate of carbon in aliphatics made by Wickramasinghe & Allen (1980) based on their spectrum of GC IRS 7 and is slightly lower than the 30%–50% range derived by Schutte (1988).

Accounting for this aliphatic material exclusively with complex organics implies that at least 65% of the carbon in the diffuse medium is in other carbonaceous materials including aromatic molecules and amorphous carbon particles. Strong, infrared emission features near 3040, 1615, 1300, 1150, and 890  $\text{cm}^{-1}$  (3.29, 6.2, 7.8, 8.7, and 11.2  $\mu\text{m}$ ) from different objects suggest that aromatic hydrocarbons exist in many galactic environments. It might thus be expected that an absorption feature due to the aromatic C-H stretch should be apparent in these spectra near 3040  $\text{cm}^{-1}$  (3.3  $\mu\text{m}$ ). However, the absolute strength of the C-H stretching feature per hydrogen atom is typically 2–3 times weaker in aromatics than in saturated aliphatics (Gribov & Smirnov 1962; Wexler 1967; Bishop & Cheung 1982). Because of the relative weakness of the aromatic C-H stretch, these spectra do not provide a sensitive probe for aromatics. The amount of carbon determined to be present in molecular interstellar polycyclic aromatic hydrocarbon molecules using other techniques is on the order of a few percent (Allamandola, Tielens, & Barker 1989). This is consistent with the lack of detection of a well defined aromatic C-H absorption feature in our spectra near 3040  $\text{cm}^{-1}$  (3.3  $\mu\text{m}$ ). This also bears

on the analysis of the C-H band carrier by Adamson et al. (1990). They model the band as being produced by HAC and conclude that the material has a very high degree of hydrogenation. The hydrogen-to-carbon ratio they deduce is 0.8. If the hydrogen is evenly dispersed throughout the HAC particles, then nearly every carbon atom will be attached to a hydrogen atom. This situation is impossible for material made entirely of aromatic building blocks and the presence of aliphatics as side chains on the aromatic structural units in HAC is required.

Finally, the data do not presently indicate any clear relationship between the interstellar hydrocarbon and silicate components. Of the objects for which we have good C-H feature optical depths, only a few have reported values for  $\tau$  in the silicate band. Measurements of the relative optical depths of these two features will have to be made for additional objects before it is possible to address the relationship between the interstellar aliphatic and the silicate components.

## 5. CONCLUSIONS

In an attempt to better constrain and quantify the composition of the material in the diffuse interstellar medium, we have taken absorption spectra between 3600 and 2700  $\text{cm}^{-1}$  (2.8 and 3.7  $\mu\text{m}$ ) of a number of objects along different lines of sight which suffer differing amounts of visual extinction. The spectra of these objects generally contain either a broad feature centered near 3300  $\text{cm}^{-1}$  (3.0  $\mu\text{m}$ ), a broad feature near 2950  $\text{cm}^{-1}$  (3.4  $\mu\text{m}$ ), or both.

The 3300  $\text{cm}^{-1}$  feature is attributed to O-H stretching vibrations; the 2950  $\text{cm}^{-1}$  feature is attributed to C-H stretching vibrations. The lack of correlation between the strengths of these two bands indicates that they do not arise from the same carrier. The O-H feature in OH 32.8–0.3 is suggestive of circumstellar water ice and is probably not due to material in the diffuse ISM. The spectra of GC IRS 7, OH 01–477, and T629–5 show an O-H feature which is distinct from that of OH 32.8–0.3. Our spectra do not presently allow us to determine whether this feature originates from diffuse ISM dust or from more localized material.

The features in the 3100–2700  $\text{cm}^{-1}$  (3.2–3.7  $\mu\text{m}$ ) spectral region fall into one of two classes. We attribute one class of features to C-H vibrations in material in the diffuse ISM on the basis of the similarity between the band profiles along the very different lines of sight to GC IRS 7 and VI Cygni #12. Similar features are also reported for GC IRS 3, Ve 2–45, and AFGL 2179. The second class of features are associated with M stars. The high-resolution spectra of the M stars we have observed show a series of narrow features in this region that we identify with photospheric OH. Objects in which these bands are seen include OH 01–477, T629–5, and the Galactic center source IRS 7 (very weakly). These features can make the detection of absorption bands from diffuse interstellar materials very difficult and M stars are best avoided for studies of the diffuse medium at these wavelengths.

The C-H stretch feature of diffuse ISM dust has subpeaks near 2955, 2925, and 2870  $\text{cm}^{-1}$ , all of which fall within 5  $\text{cm}^{-1}$  of C-H stretching vibrations in the  $-\text{CH}_2-$  and  $-\text{CH}_3$  groups of saturated aliphatic hydrocarbons. For GC IRS 7, the object for which we have the best higher resolution data, these band positions fall within 1 part in 500 of three of the four standard aliphatic positions. The lack of a fourth aliphatic band near 2855  $\text{cm}^{-1}$  in the spectrum of GC IRS 7 suggests that the aliphatic material in the diffuse ISM contains small amounts of

electronegative groups. The relative strengths of these subpeaks suggests that the material in the diffuse interstellar medium has a line-of-sight average  $-\text{CH}_2/-\text{CH}_3$  ratio of about 2.5. Thus, the material responsible contains short chain organic materials. The strength of the subpeaks at 2925 and 2955  $\text{cm}^{-1}$ , due to  $-\text{CH}_2-$  and  $-\text{CH}_3$  groups, respectively, correlate with visual extinction, strongly suggesting that the C-H stretching band is a general feature of the material along different lines of sight in the diffuse ISM. We find average ratios of  $A_{\nu}/\tau_{(2925\text{ cm}^{-1})} = 240 \pm 40$  and  $A_{\nu}/\tau_{(2955\text{ cm}^{-1})} = 310 \pm 90$  for the objects we have observed. From the strength of the observed features, we deduce that the percent of cosmic carbon in the ISM that is tied up in the carrier of this band lies between 2.6% and 35%, with the most likely value falling near 10%.

Comparison of the C-H band profiles in the telescopic data

with the spectra of lab residues created by irradiating ices with compositions similar to those inferred for the ices in dense molecular clouds demonstrates remarkable similarity. This suggests that the hydrocarbon component we have observed in the diffuse interstellar medium consists in large part of complex, interlinked, aliphatic hydrocarbons that were produced in dense molecular clouds and subsequently modified in the diffuse medium.

We are especially grateful to Robert Walker for his continued expert technical support of the laboratory. We would also like to thank Sherwood Chang for kindly providing us with many of the alcohols used in our laboratory studies, Gordon Augason for calculating M star opacities, and Terry Jones for suggesting some of the objects. This work was supported by NASA grant 199-52-12-04.

#### REFERENCES

- Abbott, D. C., & Conti, P. S. 1987, *ARA&A*, 25, 113  
 Ackermann, G. 1970, *A&A*, 8, 315  
 Adamson, A. J., Whittet, D. C. B., & Duley, W. W. 1990, *MNRAS*, 243, 400  
 Allamandola, L. J. 1984, in *Galactic and Extragalactic Infrared Spectroscopy*, ed. M. Kessler & P. Phillips (Dordrecht: Reidel), p. 5  
 Allamandola, L. J., Sandford, S. A., & Valero, G. J. 1988, *Icarus*, 76, 225  
 Allamandola, L. J., Tielens, A. G. G. M., & Barker, J. R. 1989, *ApJS*, 71, 733  
 Allen, C. W. 1973, *Astrophysical Quantities* (London: Athlone)  
 Allen, D. A., & Wickramasinghe, D. T. 1981, *Nature*, 294, 239  
 Becklin, E. E., Matthews, K., Neugebauer, G., & Willner, S. P. 1978a, *ApJ*, 219, 121  
 ———. 1978b, *ApJ*, 220, 831  
 Beer, R., Hutchison, R. B., Norton, R. H., & Lambert, D. L. 1972, *ApJ*, 172, 89  
 Bishop, D. M., & Cheung, M. L. 1982, *J. Phys. Chem. Ref. Data*, 11, 119  
 Bohlin, R. C., Savage, B. D., & Drake, J. F. 1978, *ApJ*, 224, 132  
 Butchart, I., McFadzean, A. D., Whittet, D. C. B., Geballe, T. R., & Greenberg, J. M. 1986, *A&A*, 154, L5  
 Cohen, M., Tielens, A. G. G. M., & Bregman, J. D. 1989, *ApJ*, 344, L13  
 Cohen, M., & Vogel, S. N. 1978, *MNRAS*, 185, 47  
 d'Hendecourt, L. B., & Allamandola, L. J. 1986, *A&AS*, 64, 453  
 Gillett, F. C., Jones, T. W., Merrill, K. M., & Stein, W. A. 1975, *A&A*, 45, 77  
 Greenberg, J. M. 1978, in *Cosmic Dust*, ed. J. A. M. McDonnell (New York: Wiley), p. 187  
 ———. 1989, in *Interstellar Dust*, ed. L. J. Allamandola & A. G. G. M. Tielens, (Dordrecht: Kluwer), p. 345  
 Greenberg, J. M., & Chlewicki, G. 1983, *ApJ*, 272, 563  
 Greenberg, J. M., & Hong, S. S. 1974, in *ESLAB Symposium #8*, ed. A. F. M. Moorwood (ESRO SP-105), p. 153  
 Gribov, L. A., & Smirnov, V. N. 1962, *Soviet Phys.-Uspekhi*, 4, 919  
 Hagen, W., Tielens, A. G. G. M., & Greenberg, J. M. 1983, *A&AS*, 51, 389  
 Henry, J. P., DePoy, D. L., & Becklin, E. E. 1984, *ApJ*, 285, L27  
 Herman, J., Isaacman, R., Sargent, A., & Habing, H. J. 1984, *A&A*, 139, 171  
 Humphreys, R. M. 1978, *ApJS*, 38, 309  
 Jones, A. P., Duley, W. W., & Williams, D. A. 1987, *MNRAS*, 229, 213  
 Jones, T. J., Hyland, A. R., & Allen, D. A. 1983, *MNRAS*, 205, 187  
 Jones, T. J., Hyland, A. R., Caswell, J. L., & Gatley, I. 1982, *ApJ*, 253, 208  
 Lebofsky, M. J., Rieke, G. H., & Tokunaga, A. T. 1982, *ApJ*, 263, 736  
 Leitherer, C., Bertout, C., Stahl, O., & Wolf, B. 1984, *A&A*, 140, 204  
 Mathis, J. S. 1989, in *Interstellar Dust*, ed. L. J. Allamandola & A. G. G. M. Tielens (Dordrecht: Kluwer), p. 357  
 Mathis, J. S., Rimpl, W., & Nordsieck, K. H. 1977, *ApJ*, 217, 425  
 Mathis, J. S., & Whiffen, G. 1989, *ApJ*, 341, 808  
 McFadzean, A. D., Whittet, D. C. B., Longmore, A. J., Bode, M. F., & Adamson, A. J. 1989, *MNRAS*, 241, 873  
 Nugis, T. 1982, in *Wolf-Rayet Stars: Observations, Physics, Evolution*, ed. C. W. H. de Loore & A. J. Willis (Dordrecht: Reidel), p. 131  
 Pitault, A., Epchtein, N., Gomez, A. E., & Lortet, M. C. 1983, *A&A*, 120, 53  
 Ridgway, S. 1984, in *Galactic and Extragalactic Infrared Spectroscopy*, ed. M. F. Kessler, & J. P. Phillips, (Dordrecht: Reidel), p. 309  
 Rieke, G. H. 1974, *ApJ*, 193, L81  
 Rieke, G. H., Rieke, M. J., & Paul, A. E. 1989, *ApJ*, 336, 752  
 Roche, F. P., & Aitken, D. K. 1984a, *MNRAS*, 208, 481  
 Roche, F. P., & Aitken, D. K. 1984b, *MNRAS*, 209, 33p  
 Sandford, S. A., & Walker, R. M. 1985, *ApJ*, 291, 838  
 Schulte, D. H. 1958, *ApJ*, 128, 41  
 Schutte, W. A. 1988, Ph.D. thesis, Leiden University  
 Sellgren, K., Hall, D. N. B., Kleinmann, S. G., & Scoville, N. Z. 1987, *ApJ*, 317, 881  
 Silverstein, R. M., & Bassler, G. C. 1967, *Spectrometric Identification of Organic Compounds* (New York: Wiley), 2nd edition  
 Soifer, B. T., Russell, R. W., & Merrill, R. M. 1976, *ApJ*, 207, L83  
 Tapia, M. 1981, *MNRAS*, 197, 949  
 Tapia, M., Persi, P., Roth, M., & Ferrarri-Toniolo, M. 1989, *A&A*, 225, 488  
 Tielens, A. G. G. M., & Allamandola, L. J. 1987, in *Physical Processes in Interstellar Clouds*, ed. Morfill, G. E., & Scholer, M. (Dordrecht: Reidel), p. 333  
 Tielens, A. G. G. M., et al. 1991, in preparation  
 Tokunaga, A. T., ed. 1986, *IRTF Photometry Manual* (Honolulu: Univ. of Hawaii)  
 Tokunaga, A. T., Smith, R. G., & Irwin, E. 1987, in *Infrared Astronomy with Arrays*, ed. C. G. Wynn-Williams, E. E. Becklin, & L. H. Good (Honolulu: University of Hawaii), p. 367  
 Torres, A. V. 1988, *ApJ*, 325, 759  
 Torres-Dodgen, A. V., Tapia, M., & Carroll, M. 1991, *MNRAS*, in press  
 van der Zwet, G. P., Allamandola, L. J., Baas, F., & Greenberg, J. M. 1985, *A&A*, 145, 262  
 Wade, R., Geballe, T. R., Krisciunas, K., Gatley, I., & Bird, M. C. 1987, *ApJ*, 320, 570  
 Wexler, A. S. 1967, *Appl. Spectroscopy Rev.*, 1, 29  
 White, R. L., & Becker, R. H. 1983, *ApJ*, 272, L19  
 Wickramasinghe, D. T., & Allen, D. A. 1980, *Nature*, 287, 518  
 ———. 1983, *Ap&SS*, 97, 369  
 Williams, D. 1989, in *Interstellar Dust*, ed. L. J. Allamandola & A. G. G. M. Tielens (Dordrecht: Kluwer), p. 367  
 Williams, P. M., van der Hucht, K. A., & Thé, P. S. 1987, *A&A*, 182, 91  
 Willis, A. J. 1982, in *Wolf-Rayet Stars: Observations, Physics, Evolution*, ed. C. W. H. de Loore & A. J. Willis (Dordrecht: Reidel), p. 87  
 Willner, S. P., & Pipher, J. L. 1982, in *The Galactic Center*, AIP Conf. Proc. No. 83, ed. G. R. Reigler & R. D. Bladford (New York: AIP), p. 77  
 Willner, S. P., Russell, R. W., Puetter, R. C., Soifer, B. T., & Harvey, P. M. 1979, *ApJ*, 229, L65